scientific reports

OPEN

Dynamic modeling of geological carbon storage in an oil reservoir, Bredasdorp Basin, South Africa

Blessing Afolayan [1]✉, Eric Mackay [2] & Mimonitu Opuwari [1]

Geological carbon storage provides an efficient technology for the large-scale reduction of atmospheric carbon, and the drive for net-zero emissions may necessitate the future usage of oil reservoirs for CO_2 projects (without oil production), hence, dynamic modeling of an oil reservoir for CO_2 storage in the Bredasdorp basin, South Africa, was therefore conducted. Injection into the reservoir was for 20 years (2030–2050), and 100 years (2050–2150) to study the CO_2–brine–oil interactions, with sensitivities carried out on reservoir boundary conditions. The closed boundary scenario experienced pressure buildup with a target injection rate of 0.5 Mt/year, and a cutback on injection rate progressively until 2050 to not exceed the fracture pressure of the reservoir. The CO_2 plume migration was not rapid due to the reduced volume of CO_2 injected and the confining pressure. The system was gravity dominated, and gravity stability was not attained at the end of the simulation as fluid interfaces were not yet flat. The open boundary reservoir did not experience a pressure buildup because all boundaries were open, the target injection rate was achieved, and it was a viscous-dominated system. In both cases, the dissolution of CO_2 in oil and brine was active, and there was a growing increase of CO_2 fraction dissolved in water and oil, a decline in gaseous mobile CO_2 phase between 2050 and 2150, and active trapping mechanisms were structural trapping, dissolution in oil and water, and residual trapping. The study showed that boundary condition was very crucial to the success of the project, with direct impacts on injection rate and pressure. This pioneering study has opened a vista on the injection of CO_2 into an oil reservoir, and CO_2–brine–oil interactions, with sensitivities carried out on reservoir boundary conditions in a closed and an open hydrocarbon system in South Africa.

Global sea level and temperature rise (climate change) have been constantly perceived to be caused by the untoward concentration of greenhouse gases (GHGs) in the earth's atmosphere, and carbon dioxide (CO_2) the major constituent of GHGs[1–6]. Other energy sources especially renewables have received significant investments, but due to the ever-increasing demand for energy globally, fossil fuels will still be in the mix for the foreseeable future[1,7,8]. With man's continued reliance on fossil fuels, and CO_2 being a byproduct of fossil fuel combustion, drives and initiatives to mitigate the adverse effects of climate change must constantly be on the front burner. Goal 13 (climate action), one of the goals within the Sustainable Development Goals (SDGs) as adopted in 2015 by the United Nations (UN) speaks to the necessity of taking "urgent actions to combat climate change and its impact" and targets the integration of climate change strategies into national planning and policies[9,10]. Geological carbon storage is presently the most efficient technology for large-scale reduction of atmospheric carbon and stemming the upward tide of associated climate challenges, as the International Energy Agency asserts it can bring about around 19% reduction in emissions of CO_2 worldwide by 2050[11]. Yearly CO_2 emissions on a global scale from cement manufacture and burning of fossil fuels were 36.58 Giga tonnes per annum (Gtpa) in 2018, with 10.06 Gt (28% of the world's entirety) contributed by China, the USA emitted 5.42 Gt (15% of the world's total sum), and India accounted for 2.65 Gt, representing 7% of total CO_2 emission of the world[12,13]. With 28 carbon capture and storage (CCS) projects operational worldwide as of 2020 and sequestering 41 Mtpa[14], this represents a meagre 0.12% of the CO_2 emissions attributable to hydrocarbon and cement industries worldwide. About 37% of these are principally geological carbon storage projects, while 73% are for enhanced oil recovery (EOR) drives, with the USA, Brazil and, Australia being the nations that sequestered the most[13]. Some operational carbon storage projects around the world include the Gorgon Carbon Dioxide Project, Uthmaniyah CO_2-EOR

[1]Petroleum Geosciences Research Group, Department of Earth Sciences, University of the Western Cape, Bellville 7535, Republic of South Africa. [2]Institute of Petroleum Engineering, Heriot-Watt University, Riccarton, Edinburgh EH14 4AS, UK. ✉email: 3993275@myuwc.ac.za

1

project[15–17], CNPC Jilin Oil Field CO_2-EOR[18–20] and Alberta Carbon Trunk Line (ACTL) Sturgeon Refinery CO_2 Stream project[21–23]. Some under construction presently include The Sinopec Qilu Petrochemical Carbon Store Project[24,25], Guodian Taizhou Power Station Carbon Capture[26,27], Air Liquide Refinery Rotterdam CCS[28–30], The ZEROS Project[31,32] and Norcem Brevik Cement Plant[33,34] among others.

Within the South African context, studies have shown that South Africa has the potential of storing ~ 150 Gt of CO_2, with the offshore basins showing greater prospects[35–40], but it is unlikely that commercially available CCS will be in place in the country before 2030 due to the present challenges of doubts in policies around climate action, delayed pilot/test underground carbon injection projects, low-priced carbon rates, dearth of commercial or profitable case studies, and the acceptability of the public to carbon storage projects in regions hosting potential storage sites[41–47]. South Africa fulfils its energy needs principally from fossil fuels, with 77% of the nation's total electricity generation from coal-fired power plants and its power sector the 9th biggest emitter among power sectors in the world (~ 218 Mt of CO_2) (Fig. 1), though these are low emissions in comparison to developed nations, cumulative emissions from the next nine African nations are below it[48]. Preliminary studies have been carried out to identify and estimate the capacities of potential geological CO_2 reservoirs in South Africa[39], with particular focus on the Zululand basin[49], Algoa[36,50], and the Bredasdorp basin[51–53], with a pilot CO_2 injection test scheduled for 2023[54,55]. These continued inquests into underground carbon storage are a pointer that it will play a big part in the decarbonization of South Africa.

In the bid to attain climate neutrality, Denmark, currently the largest oil producer in the European Union (EU), is set to completely phase out the production of hydrocarbon, new oil and gas extraction permits have been cancelled and when the calendar reads 2050, the hydrocarbon valves will be shut off for good. Presently, subsidies are being provided to stimulate large-scale CCS projects[56,57]. This means more searchlights will be beamed on oil reservoirs (without oil recovery) to make them viable CO_2 sinks. Oil reservoirs present many advantages for CO_2 storage, such as the presence of below-surface and on-the-ground installations and equipment that can be tailored to CO_2 injection and storage (usually with some modifications), the presence of quality seal and establishment of caprock integrity which have held oil in place through geologic time, and availability of geological, hydrogeological, geophysical and engineering data for characterization of the reservoir and other petroleum system elements, among others[5,58–64].

Therefore, this research aims to consider an oil reservoir in the offshore Bredasdorp basin, South Africa, for CO_2 storage, with no enhanced oil recovery (EOR). The knowledge gained from the study will also be useful for reservoirs with pockets of unrecoverable oil due to economic, technical, commercial, or logistics reasons, and bypassed oil/unswept zones.

Methodology

With the aid of the equation-of-state CMG-GEM compositional simulator (2022.30v), dynamic simulation was conducted for CO_2 injectivity and storage in the oil reservoir, with a focus on CO_2 plume migration, active trapping mechanisms, and supercritical CO_2–oil–brine interactions. The reservoir used for this study is a clastic type with shales, siltstones, and sandstone units, and it has a permeability range of 3–560 mD and average effective porosity of 14%[51]. For CO_2 solubility in the aqueous phase, Henry's law was employed[65–69], with the formation and fluid values, as well as the composition of the oil used for the study presented in Tables 1, 2.

Two rock types were delineated in the reservoir based on permeability zones[70], namely high (rock type 1) and low (rock type 2) permeability zones, with permeability cut-off set at 150 mD as the reservoir had prevailing permeability values of 100–560 mD[51] (Fig. 2). Given three-phase flow in the reservoir (oil, CO_2, and water) and at connate water saturation, for both zones, there were liquid–gas relative permeability values[71], and water–oil relative permeability values (generated from Corey correlation)[72–76] (Fig. 3).

Dynamic simulations were carried out to simulate the injection of 0.5 Mt/year of CO_2 (762,000 m³/day) in the oil reservoir for 20 years (2030–2050) with one injection well, and a further simulation period of 100 years (2050–2150) to study the CO_2–oil–brine interactions. Two scenarios were considered based on the boundary conditions of the reservoir, namely (i) open system (all boundaries open); and (ii) closed system (all boundaries closed).
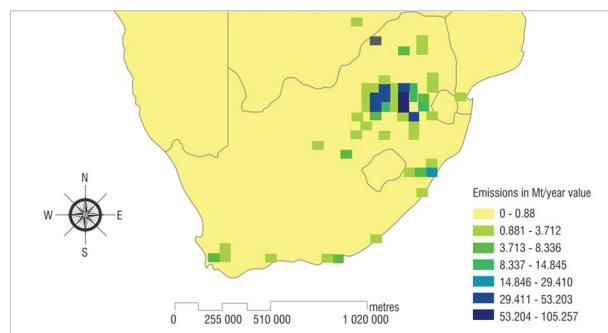

Figure 1. Core point sources of carbon dioxide emissions in South Africa are in the Free State, Gauteng, and Mpumalanga provinces hosting the coal mines and most of the coal-fired power plants. Emissions from oil refineries, gas-to-liquid, and coal-to-liquid firms are also covered here. Adapted after[48].

| Reservoir and fluid properties	Values
Type of reservoir	Sandstone
Maximum thickness (m)	77
Depth of reservoir top (m)	2622
Pressure at reservoir depth (kPa)	26,153
Temperature at reservoir depth (°C)	110
Rock compressibility (kPa)	5.29×10^{-7}
Maximum bottom hole pressure (kPa)	30,000
Number of injection wells	1
Model discretization	$89 \times 72 \times 40$
Total blocks	256,320
Number of active blocks	240,892
Water density (kg/m^3)	1010
Rate of injection (m^3/day)	762,000
Irreducible water saturation (rock type 1)	0.144
Irreducible water saturation (rock type 2)	0.294
Residual oil saturation (rock type 1)	0.423
Residual oil saturation (rock type 2)	0.326
Permeability cut-off for rock type (mD)	150

Table 1. Reservoir and fluid values.

Composition	Molar fraction
CH_4	21.33
C_2H_6	7.39
C_3H_8	6.05
C_4H_{10}	2.41
C_5H_{12}	3.44
C_6H_{14}	3.37
C_7H_{16}–$C_{13}H_{28}$	30.18
$C_{14}H_{30}$–$C_{20}H_{42}$	10.7
$C_{21}H_{44}$–$C_{28}H_{58}$	5.55
$C_{29}H_{60}$+	9.57

Table 2. Oil composition.
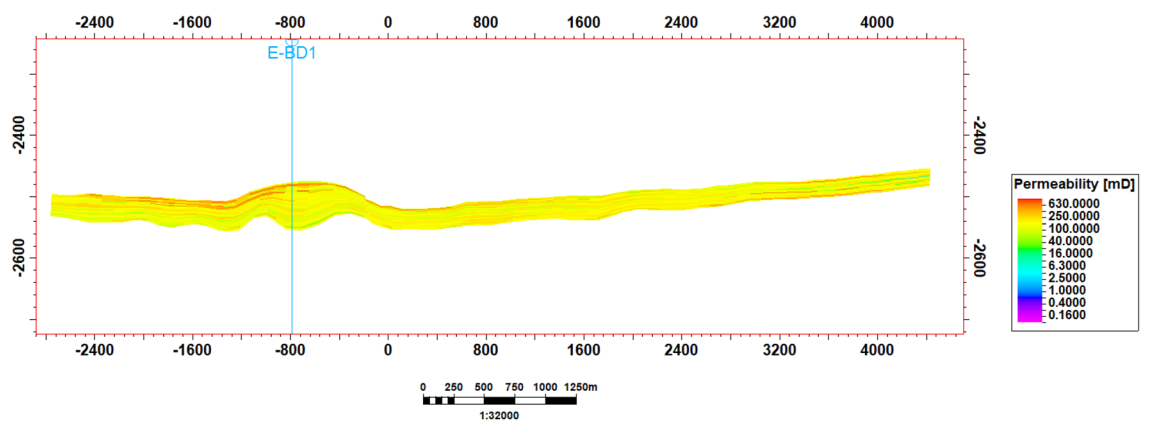
Figure 2. EW cross-sectional view of permeability distribution in the reservoir.
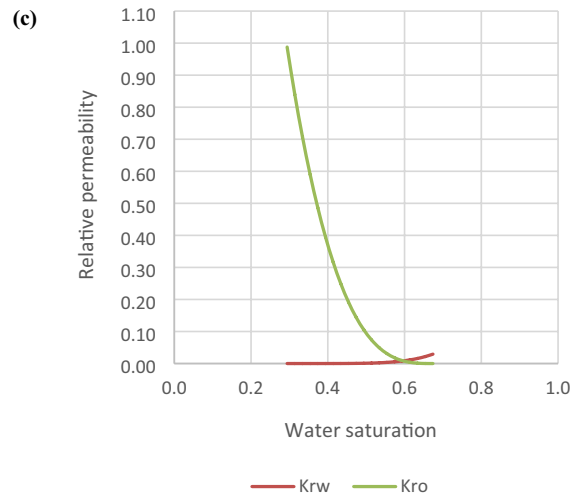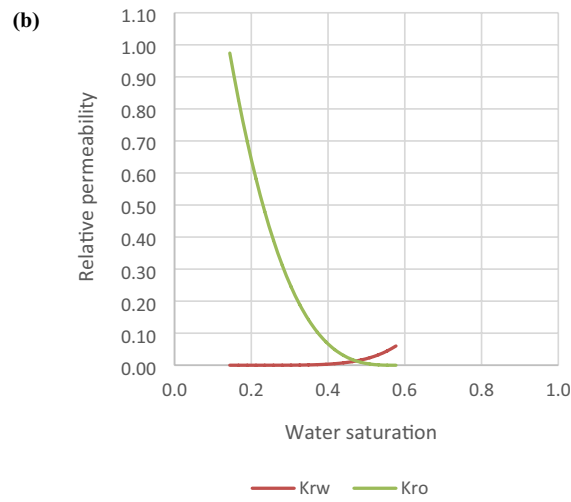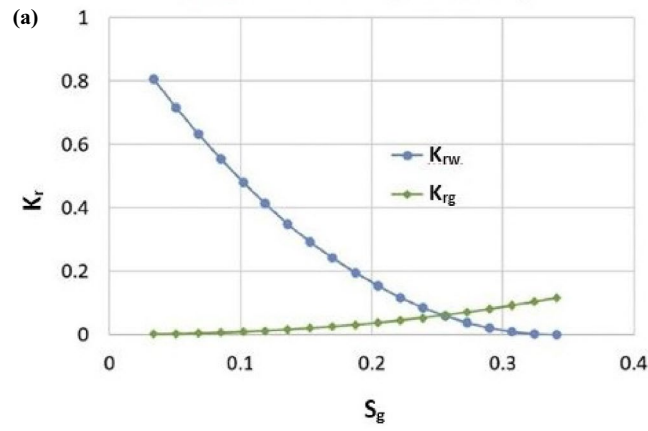
Figure 3. (**a**) Liquid–gas relative permeability curve; (**b**) water–oil relative permeability curve for high permeability zones and (**c**) water–oil relative permeability curve for low permeability zones.

Results and discussion
Closed boundary system
Injection and pressure
The maximum allowable pressure (well bottom-hole pressure, BHP) in the reservoir was set at 30,000 kPa, equivalent to 90% of reservoir lithostatic pressure[77,78]. With the target gas rate set at 0.5 Mt/year (762,000 m^3/day) and the inability of pressure to dissipate in the system due to closed reservoir boundaries, the plot of BHP against time (Fig. 4) showed a steadily rising gas rate until it reached the maximum rate allowable (653,649 m^3/day) to not exceed the maximum pressure, then the injection/gas rate was cut back to ensure caprock was not damaged. The average reservoir pressure rose from 25,500 kPa at the onset of injection in 2030, peaked at 30,000 kPa in 2050 and this pressure was maintained from 2050 to 2150. BHP and Well block pressure dropped to 29,741 kPa in 2050 to 2150, as the pressure due to injection of CO_2 into the reservoir had ceased.

In any underground carbon storage project, a target amount of CO_2 is proposed for injection into the ground, usually accompanied by pressure buildup in the system. The attainment of this desired injection rate is dependent on the injectivity of the reservoir, as an injection rate that is too high can cause the downhole pressure to exceed the fracture pressure, inducing reservoir and seal fracturing, or reactivation of existing sealing faults, all leading to environmental concerns[64]. A typical project that has had to deal with this scenario is the CO_2 injection into the Tubåen Formation at Snøhvit, where a considerable rate of pressure at the early onset of the project led to cutting down of injection rates, and subsequent abandonment of injection into the formation when the pressure increase considerably approached the fracture pressure[79–81].

CO_2 plume migration and active flow regime
CO_2 plume did not migrate rapidly away from the wellbore due to confining pressure, and reduction in the volume of CO_2 injected into the reservoir with the inability to attain the intended constant injection rate of 0.5 Mt/year (Fig. 5a,c). Supercritical CO_2 accumulated at the top of the reservoir due to buoyancy in 2150, rather than moving rapidly laterally (Fig. 5b,d)[82]. The system was gravity dominated, as counter-current movement ensued in the vertical route owing to the gravity segregation of CO_2, water, and oil, and the CO_2 invasion into the reservoir being stable due to gravity stability and gravity exceeding viscous forces[83], it is also pertinent to note that low injection rate is accompanied with less lateral spreading of gas[84]. Though the gravity segregation was reduced because of relative permeability[85–88], with increasing residence time, the system will be fully gravity stable evidenced by fluid interfaces being flat, as interfaces are usually destabilized by viscous forces[83]. There was structural trapping under the caprock, and the occurrence of non-reservoir rocks also provided local compartmentalization in the reservoir, aiding the reduction of the rapid migration of the plume.

*CO_2 dissolution in oil and brine*
Displacement of oil by injected CO_2 is active in the reservoir, though only 71% of the oil can be displaced (Fig. 6a), the heavier hydrocarbon components (29%) are not dissolved into the gas phase. Oil mass density (Fig. 6b) ranged from 650 kg/m^3 in the CO_2 uninvaded zones to 699 kg/m^3 in the zones invaded by CO_2, with water mass density (Fig. 6c) also increasing to 1031 kg/m^3 in blocks that CO_2 had invaded. This indicates active dissolution of CO_2 in the reservoir fluids, as formation fluids density increases progressively as they become enriched with CO_2[89,90].
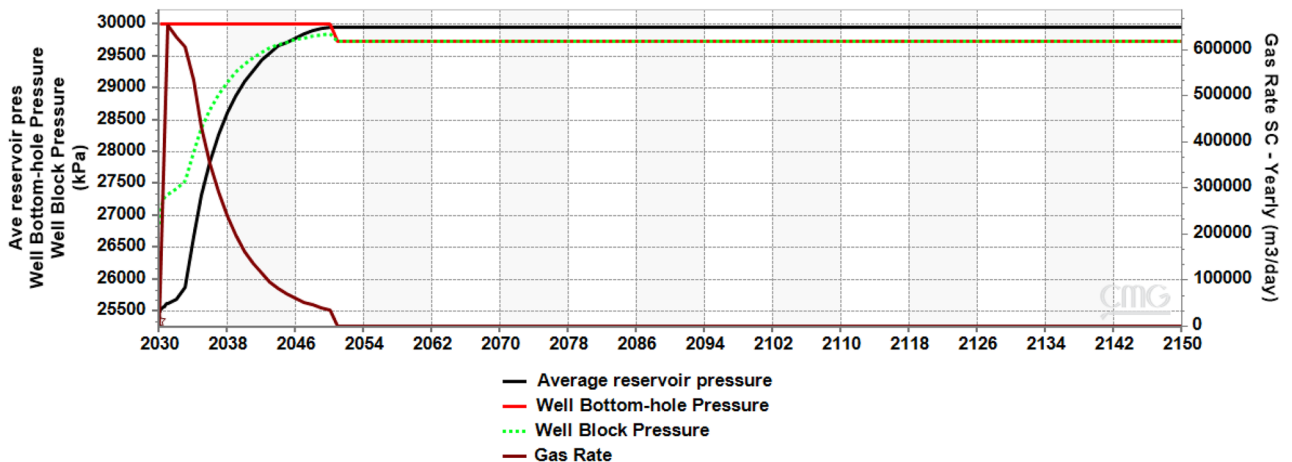
Figure 4. Cross-plot of average reservoir pressure, well bottom-hole pressure, well block pressure and gas rate.

(a)

(b)

(c)
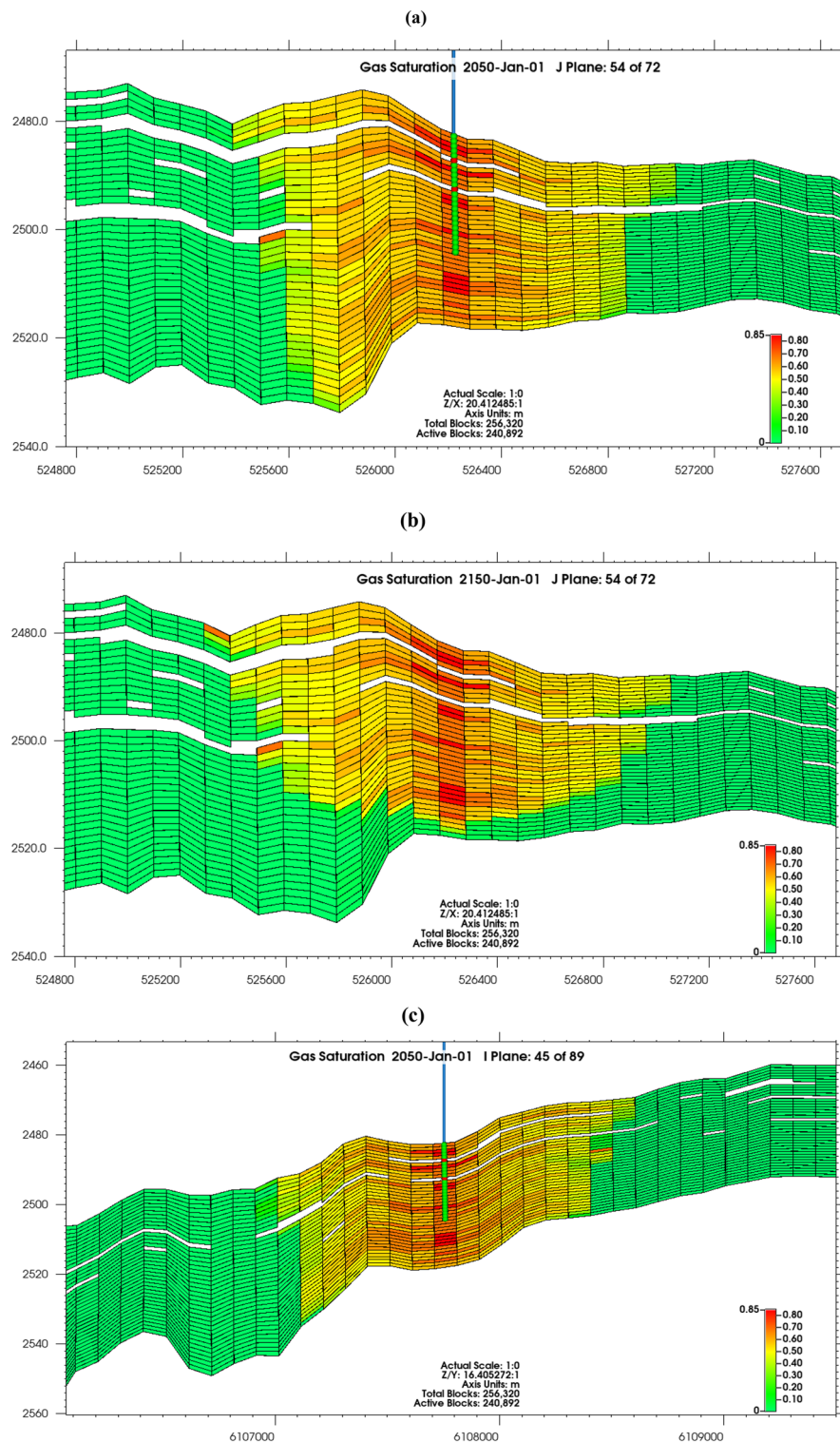
Figure 5. Gas saturation profile from (**a**) J plane after 20 years of injection (2050), (**b**) J plane at 100 years of storage (2150), (**c**) I plane after 20 years of injection (2050), (**d**) I plane at 100 years of storage (2150).
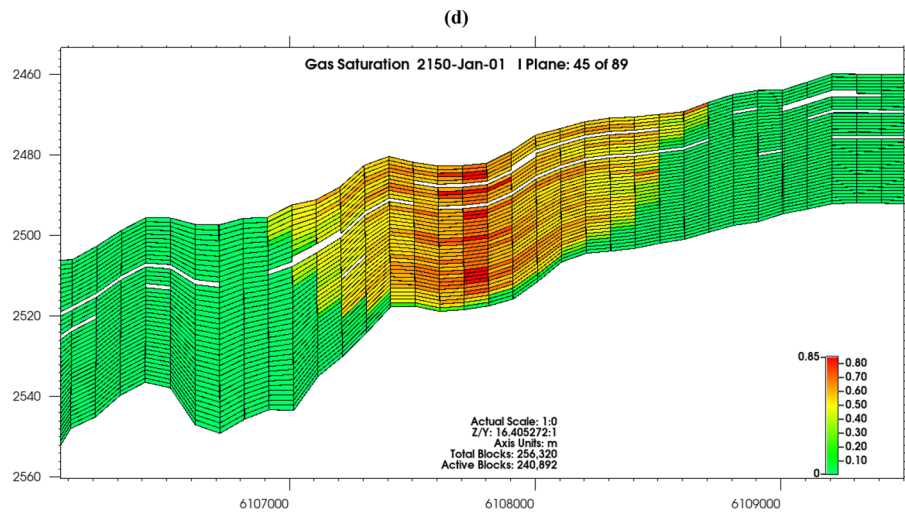
Figure 5. (continued)

Active trapping mechanism
Active CO_2 trapping mechanisms were structural trapping under the caprock (supercritical mobile), dissolution and residual trapping (Fig. 7a,c). At the end of injection in 2050, 74.9 billion moles (3.3 Mt) of CO_2 had been successfully injected into the reservoir, 63.7% was in the gaseous mobile phase, 27.7% had dissolved in oil, 4% was trapped residually and 4.5% had dissolved in brine (Fig. 7b,c). In 2150, 4.8% had dissolved in water, 35.9% dissolved in oil, 3.6% was trapped residually and 55.5% was in the gaseous mobile phase.

There was a growing increase in CO_2 fraction dissolved in oil and water and a decline in the residually trapped and gaseous mobile CO_2 phase. With further residence time, which is a core element of the CO_2 storage process[91–93], this trend should continue.

Open boundary system
Injection and pressure
With all boundaries open, there was pressure dissipation in the system. In Fig. 8, the average reservoir pressure was constant at 25,395 kPa from 2030 to 2150, maximum well bottom-hole pressure recorded was 31,000 kPa in 2050, which was below the lithostatic pressure of the formation (33,440 kPa). The pressure dropped to 25,290 kPa after cessation of injection, which was maintained till 2150. Well block pressure rose from 26,000 kPa in 2030 to 26,297 kPa in 2050 and dropped to 25,290 kPa from 2050 to 2150. Pressure dissipation in the system because of open boundaries also ensured the proposed gas injection rate of 762,000 m^3/day (0.5 Mt/year) was fully attained, with no direct risks of caprock and reservoir fracture, or storage capacity destruction of the rock[94].

CO_2 plume migration and active flow regime
There was gradual and active lateral migration of injected CO_2 away from the injection well (Fig. 9a–d), as there was no confining pressure in the reservoir. The system was viscous-dominated as increased injection rates were accompanied by increasing viscous forces[95], though gravity was also active, as shown by up-dip move-ment (Fig. 9c,d) and vertical segregation of the CO_2 plume from the bottom of the reservoir due to buoyancy, with supercritical CO_2 accumulating and moving directly below the seal but did not get to the reservoir flanks (Fig. 9b,d).
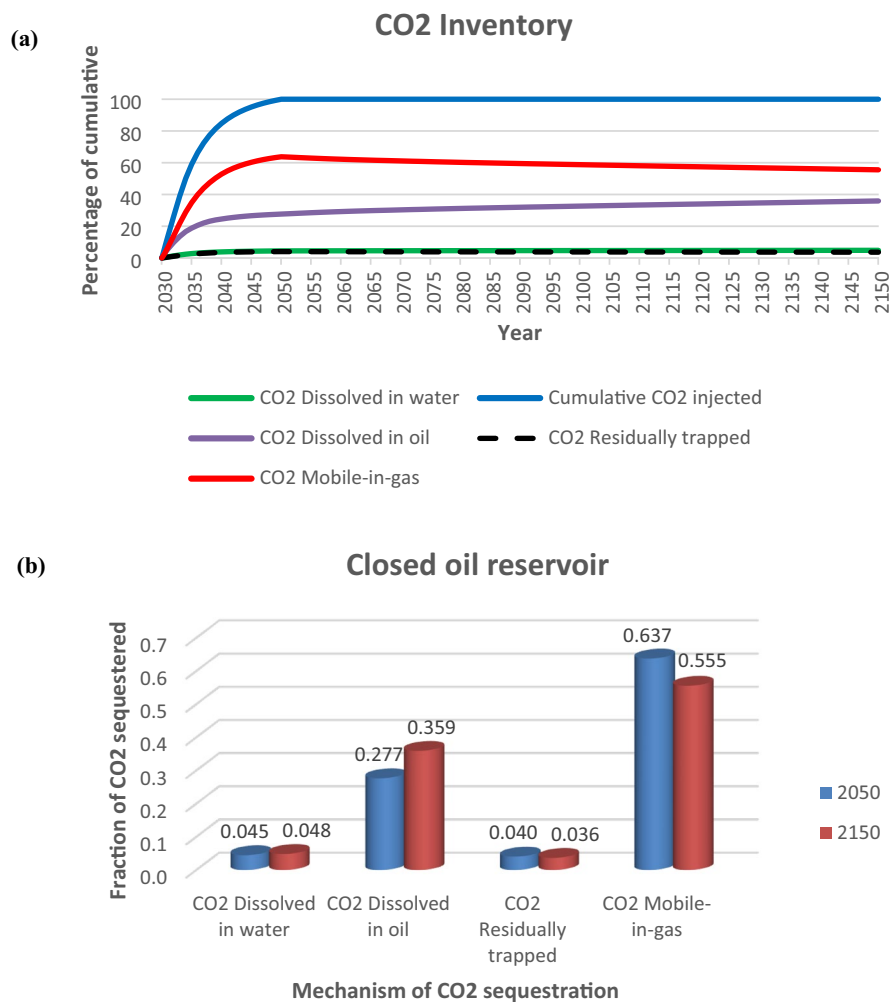
CO_2 dissolution in oil and brine
Oil displacement by injected CO_2 was active in the reservoir, though only 70.5% of the oil could be displaced (Fig. 10a), the heavier hydrocarbon components (29.5%) are not dissolved into the gas phase. Oil mass density (Fig. 10b) ranged from < 640 kg/m^3 in the CO_2 uninvaded zones to 695 kg/m^3 in the zones invaded by CO_2, with water mass density (Fig. 10c) also increasing from 1021 kg/m^3 in uninvaded zones to 1030 kg/m^3 in blocks that CO_2 had invaded. This is indicative of the active dissolution of CO_2 in the reservoir fluids, as formation fluids density increases progressively as they become CO_2 enriched[89,90].
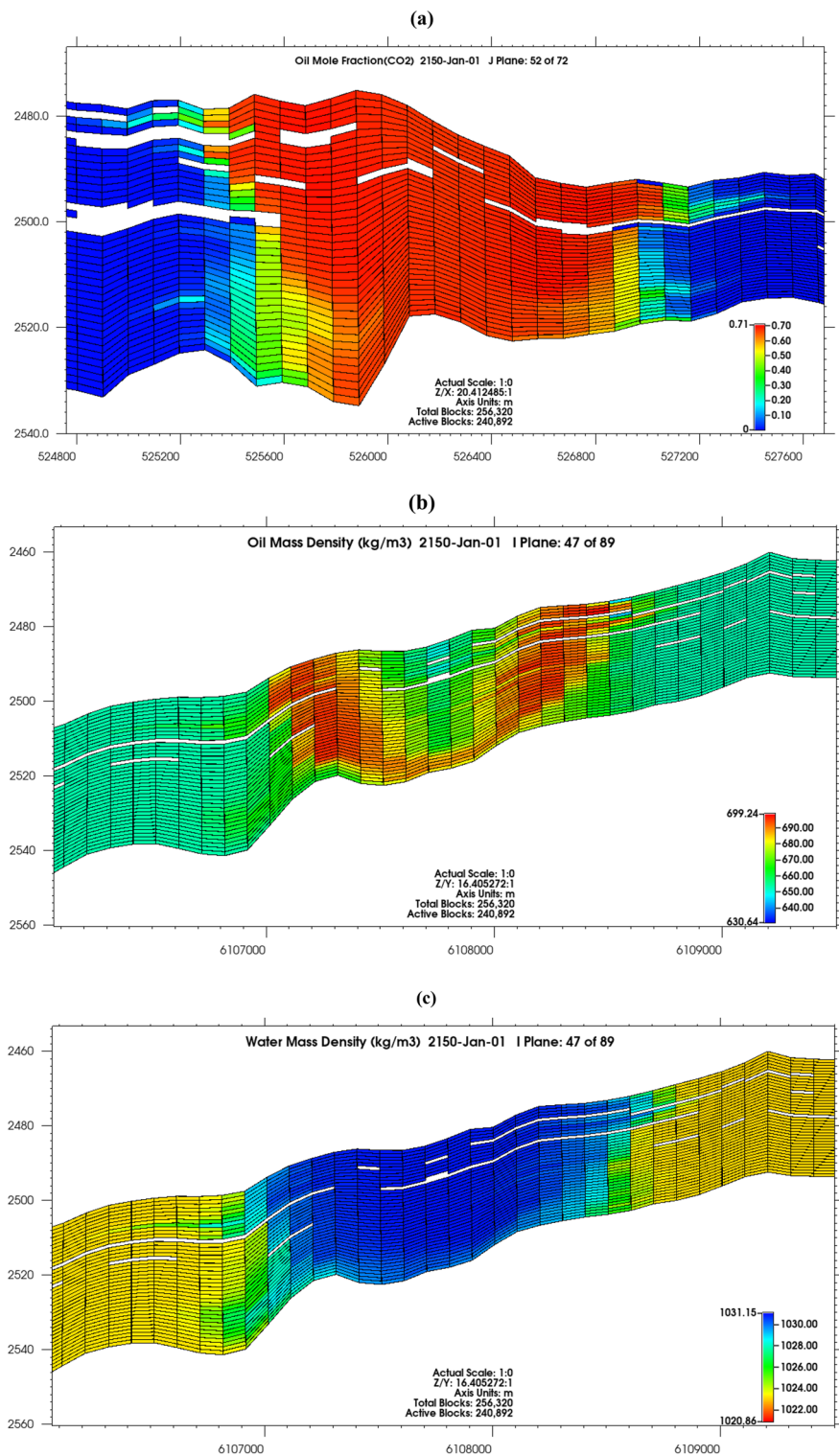
Figure 6. (**a**) Oil mole fraction of CO_2 in 2150; (**b**) Oil mass density in 2150; (**c**) Water mass density in 2150.

(a)

CO2 Inventory

- CO2 Dissolved in water
- CO2 Dissolved in oil
- CO2 Mobile-in-gas
- Cumulative CO2 injected
- CO2 Residually trapped

(b)

Closed oil reservoir

Mechanism of CO2 sequestration

(c)

Date	Cumulative Injected CO$_2$		Dissolved in water		Dissolved in oil		Mobile-in-gas		Residually trapped	
	Million tonnes	% of cumulative	Million tonnes	% of cumulative	Million tonnes	% of cumulative	Million tonnes	% of cumulative	Million tonnes	% of cumulative
2040	2.79E06	84.8	1.26E05	3.8	8.09E05	24.5	1.74E06	52.8	1.14E05	3.5
2050	3.30E6	100	1.47E05	4.5	9.12E05	27.7	2.10E06	63.8	1.32E05	4.0
2100	3.30E6	100	1.54E05	4.7	1.08E06	32.7	1.94E06	58.8	1.25E05	3.8
2150	3.30E6	100	1.59E05	4.8	1.18E06	35.9	1.83E06	55.5	1.20E05	3.6

Figure 7. (**a**) CO_2 trapping mechanism, (**b**) fraction of CO_2 sequestered, (**c**) summary of volumes of CO_2 injected, and in different trapping mechanisms.
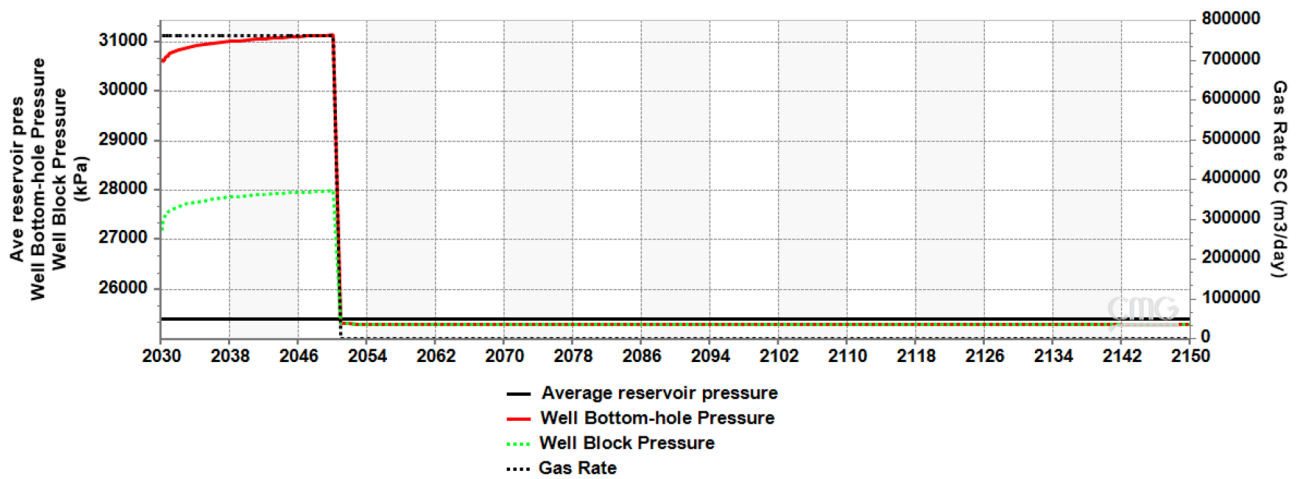
Figure 8. Cross-plot of gas rate, average reservoir pressure, well block pressure and well bottom-hole pressure.

Active trapping mechanism

Active CO_2 trapping mechanisms were structural trapping under the caprock (supercritical mobile), dissolution in oil and brine, and residual trapping (Fig. 11a,c). At the end of injection in 2050, 236 billion moles (10.4 Mt) of CO_2 had been successfully injected into the reservoir, 67.9% was in the gaseous mobile phase, 22.8% had dissolved in oil, 4.3% was trapped residually and 4.3% had dissolved in brine (Fig. 11b,c). In 2150, 4.7% had dissolved in water, 29.2% dissolved in oil, 4.2% was trapped residually and 61.7% was in the gaseous mobile phase.
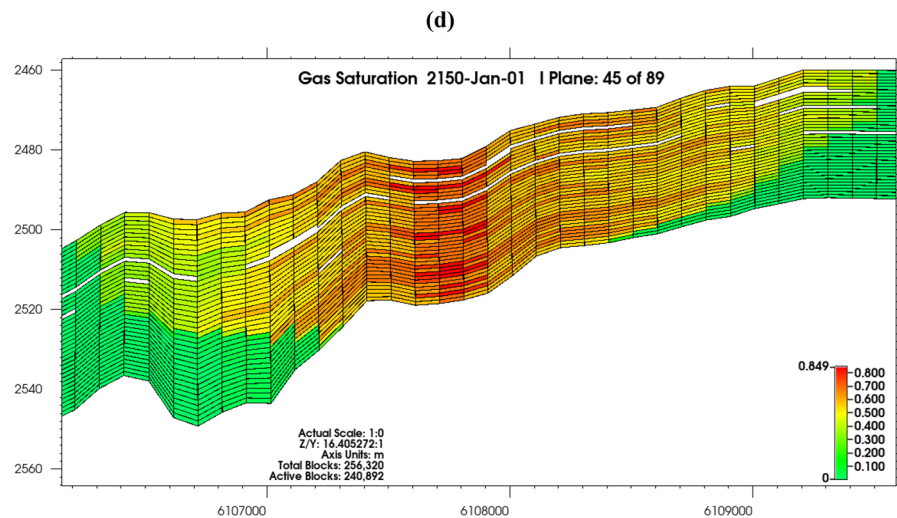
There was a gradual decline in the gaseous mobile CO_2 phase and an increase in the CO_2 fraction dissolved in oil and water. This leaning should continue upon further residence time, and a marked increase in CO_2 dissolution in water occasioned by an influx of brine into the reservoir.

Conclusion

In this study, an oil reservoir in the offshore lying Bredasdorp basin, South Africa, has been considered for CO_2 storage, without enhanced oil recovery (EOR). The closed boundary scenario experienced a pressure buildup with a target injection rate of 0.5 Mt/year, and therefore a cutback on injection rate progressively until 2050 to ensure the reservoir and overlying seal were not damaged. Migration of the CO_2 plume was not rapid, due to the reduced volume of CO_2 that was injected and confining state of the reservoir, the system was gravity dominated but did not attain gravity stability at the end of the simulation. There was a growing increase of CO_2 fraction dissolved in water and oil and a decline in the gaseous mobile CO_2 phase between 2050 and 2150. In 2150, 4.8% had dissolved in water, 35.9% dissolved in oil, 3.6% was trapped residually and 55.5% was in the gaseous mobile phase. The open boundary state experienced no pressure buildup in the reservoir and the target injection rate of 0.5 Mt/year was achieved, and 10.4 Mt of CO_2 had been successfully injected into the reservoir. CO_2 plume
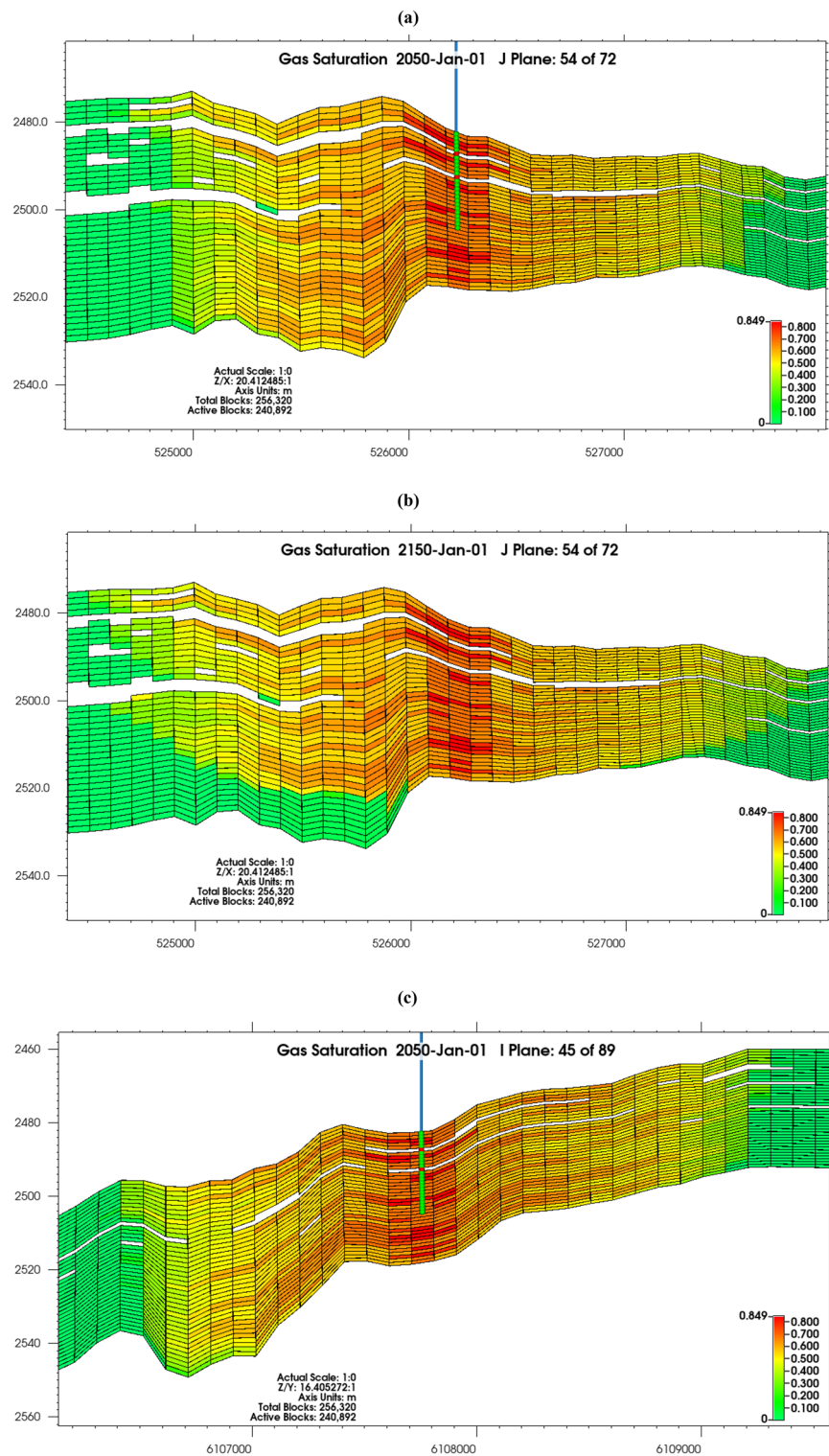
Figure 9. (**a**) Gas saturation shown from the J plane after 20 years (at 2050), (**b**) gas saturation in 2150 shown from the J plane, (**c**) gas saturation shown from the I plane after 20 years (at 2050), and (**d**) gas saturation in 2150 shown from the I plane.
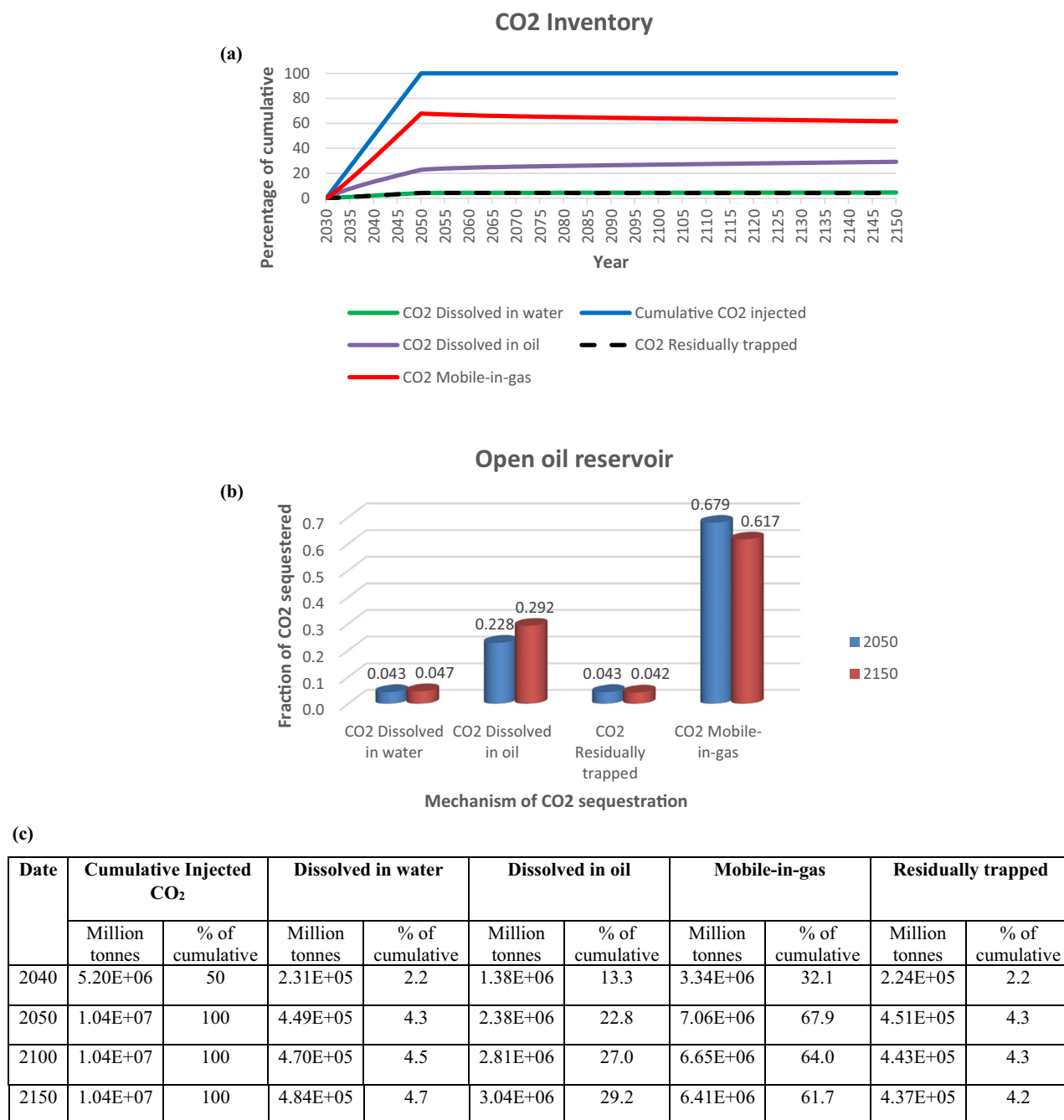
(d)

Figure 9. (continued)

migrated up-dip without getting to the reservoir flanks, it was a viscous-dominated system attended with gravity movement and segregation. With an increase in the density of formation fluids, the dissolution of CO_2 in brine and oil was active, active trapping mechanisms were structural trapping, dissolution in oil and water and residual trapping. There was a decline in the gaseous mobile CO_2 phase and an increase in CO_2 fraction dissolved in oil and water between 2050 and 2150.

With further residence time, fractions of CO_2 dissolved in the oil and brine phases would increase, as well as residually trapped fractions, with the CO_2 gaseous mobile phase experiencing a continuous decline. Therefore, this study showed that boundary condition was key to the success of the project, as it impacts injection rate and pressure.

(a)

(b)

(c)
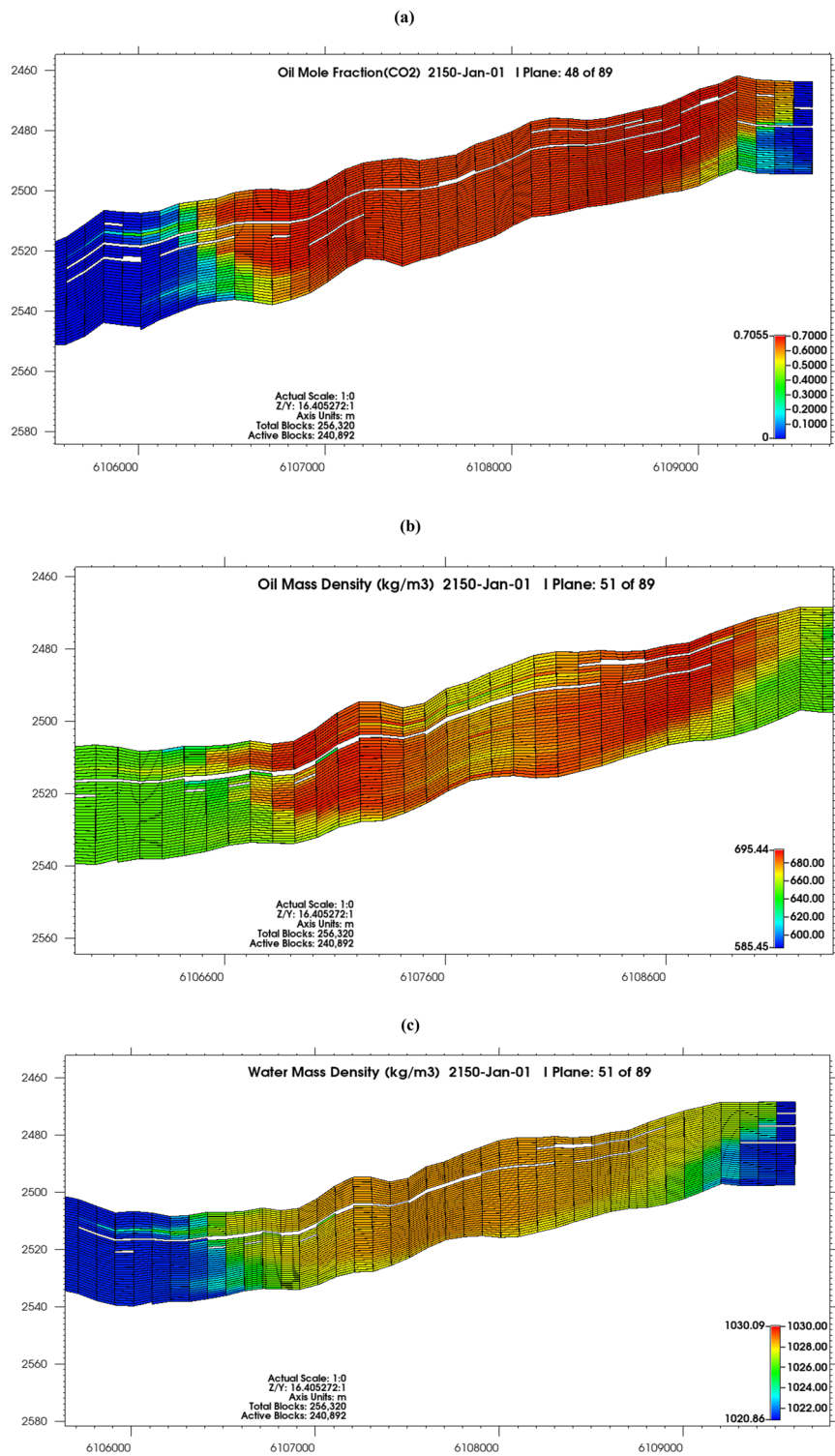
Figure 10. (**a**) Oil mole fraction of CO_2 in 2150; (**b**) oil mass density in 2150; (**c**) water mass density in 2150.

CO2 Inventory

(a)

Open oil reservoir

(b)

(c)

Date	Cumulative Injected CO₂		Dissolved in water		Dissolved in oil		Mobile-in-gas		Residually trapped	
	Million tonnes	% of cumulative	Million tonnes	% of cumulative	Million tonnes	% of cumulative	Million tonnes	% of cumulative	Million tonnes	% of cumulative
2040	5.20E+06	50	2.31E+05	2.2	1.38E+06	13.3	3.34E+06	32.1	2.24E+05	2.2
2050	1.04E+07	100	4.49E+05	4.3	2.38E+06	22.8	7.06E+06	67.9	4.51E+05	4.3
2100	1.04E+07	100	4.70E+05	4.5	2.81E+06	27.0	6.65E+06	64.0	4.43E+05	4.3
2150	1.04E+07	100	4.84E+05	4.7	3.04E+06	29.2	6.41E+06	61.7	4.37E+05	4.2

Figure 11. (**a**) CO_2 trapping mechanism, (**b**) fraction of CO_2 sequestered, (**c**) summary of volumes of CO_2 injected, and in different trapping mechanisms

References

1. Farajzadeh, R., Eftekhari, A. A., Dafnomilis, G., Lake, L. W. & Bruining, J. On the sustainability of CO_2 storage through CO_2 enhanced oil recovery. *Appl. Energy* **261**, 114467–114745 (2012).
2. Tkemaladze, G. S. & Makhashvili, K. A. Climate changes and photosynthesis. *Ann. Agrar. Sci.* **14**, 119–126 (2016).

3. IPCC. IPCC report Global warming of 1.5°C. *Glob. Warm. 1.5°C. An IPCC Spec. Rep. impacts Glob. Warm. 1.5°C above pre-industrial levels Relat. Glob. Greenh. gas Emiss. pathways, Context Strength. Glob. response to Threat Clim. Change* **2**, 17–20 (2018).
4. Ginbo, T., Di Corato, L. & Hoffmann, R. Investing in climate change adaptation and mitigation: A methodological review of real-options studies. *Ambio* https://doi.org/10.1007/s13280-020-01342-8 (2020).
5. Fagorite, V. I., Onyekuru, S. O., Opara, A. I. & Oguzie, E. E. The major techniques, advantages, and pitfalls of various methods used in geological carbon sequestration. *Int. J. Environ. Sci. Technol.* **20**, 4585–4614 (2022).
6. Zhao, K. *et al.* Recent advances and future perspectives in carbon capture, transportation, utilization, and storage (CCTUS) technologies: A comprehensive review. *Fuel* **351**, 128913 (2023).
7. Petroleum, B. *BP Energy Outlook 2035* (BP Stats, 2014).
8. Mohr, S. H., Wang, J., Ellem, G., Ward, J. & Giurco, D. Projection of world fossil fuels by country. *Fuel* https://doi.org/10.1016/j.fuel.2014.10.030 (2014).
9. UN. *Department of Economic and Social Affairs* (United Nations, 2014).
10. United Nations: Department of Economic and Social Affairs. #Envision2030 Goal 13: Climate Action | United Nations Enable. *United Nations* https://www.un.org/development/desa/disabilities/envision2030-goal13.html (2020).
11. Cao, C. *et al.* A review of CO_2 storage in view of safety and cost-effectiveness. *Energies* **13**, 600 (2020).
12. Ritchie, H., Roser, M. & Rosado, P. CO_2 and greenhouse gas emissions. *Our world data* (2020).
13. Li, H., Lau, H. C., Wei, X. & Liu, S. CO_2 storage potential in major oil and gas reservoirs in the northern South China Sea. *Int. J. Greenh. Gas Control* **108**, 103328 (2021).
14. Global CCS Institute. Global Status of CCS (2020).
15. Saini, D. Simultaneous CO_2-EOR and storage projects. In *Springer Briefs in Petroleum Geoscience and Engineering* 11–19 (Springer Nature, 2017).
16. Weyand, K., Haider, B. A. & Zhang, L. A young professional's guide to lucky no. 7: A tale of oil in the Saudi Arabian Desert. *W. Ahead* **11**, 35–36 (2015).
17. Liu, H., Consoli, C. & Zapantis, A. Overview of carbon capture and storage (CCS) facilities globally. *SSRN Electron. J.* https://doi.org/10.2139/ssrn.3366353 (2020).
18. Hill, L. B., Li, X. C. & Wei, N. CO_2-EOR in China: A comparative review. *Int. J. Greenh. Gas Control* **103**, 103173. https://doi.org/10.1016/j.ijggc.2020.103173 (2020).
19. Song, X., Wang, F., Ma, D., Gao, M. & Zhang, Y. Progress and prospect of carbon dioxide capture, utilization and storage in CNPC oilfields. *Pet. Explor. Dev.* **50**, 229–244 (2023).
20. Yuan, S. *et al.* Progress and prospects of carbon dioxide capture, EOR-utilization and storage industrialization. *Pet. Explor. Dev.* **49**, 955–962 (2022).
21. Heal, K. & Kemp, T. North west sturgeon refinery project overview—Carbon capture through innovative commercial structuring in the Canadian oil sands. In *Energy Procedia* Vol. 37 7046–7055 (Elsevier, 2013).
22. Novak Mavar, K., Gaurina-Međimurec, N. & Hrnčević, L. Significance of enhanced oil recovery in carbon dioxide emission reduction. *Sustainability (Switzerland)* **13**, 1–27. https://doi.org/10.3390/su13041800 (2021).
23. Zhang, K., Lau, H. C. & Chen, Z. Regional carbon capture and storage opportunities in Alberta, Canada. *Fuel* **322**, 124224 (2022).
24. Guo, Y. *et al.* The influence of narrative versus statistical evidence on public perception towards CCS in China: Survey results from local residents in Shandong and Henan provinces. *Int. J. Greenh. Gas Control* **84**, 54–61 (2019).
25. Meng, X. L. Low-carbon development strategy and CCS/CCUS practices of Sinopec. *Carbon Manag. Technol. Conf. 2015 Sustain. Econ. CCUS Options C.* **2**, 1031–1036 (2015).
26. Garcia, M. D. Maximum carbon dioxide capture, sequestration and maximum carbon dioxide beneficial reuse at the optimal cost efficiency for the power generation sector to address global temperature rise (2021).
27. Restrepo-Valencia, S. & Walter, A. CO_2 capture in a thermal power plant using sugarcane residual biomass. *Energies* **16**, 4570 (2023).
28. de Haas, J. & van Dril, T. Decarbonisation Options for the Industry Cluster Botlek/Pernis Rotterdam (2022).
29. Cioli, M., Schure, K. M. & Van Dam, D. Decarbonisation options for the Dutch industrial gases production. Manufacturing Industry Decarbonisation Data Exchange Network Decarbonisation options for the Dutch industrial gases production (2021).
30. Oliveira, C. & Schure, K. M. Decarbonisation options for the Dutch dairy processing industry. *PBL Netherlands Environ. Assess. Agency; TNO* 63 (2020).
31. Joseph, E. T. *et al.* Carbon sequestration: Capture, storage and utilization of CO_2 emissions from anthropogenic sources. *AIP Conf. Proc.* **2521** (2023).
32. Page, B. *et al.* The Global Status of CCS 2020: Vital to Achieve Net Zero (2020).
33. Hägg, M. B., Lindbråthen, A., He, X., Nodeland, S. G. & Cantero, T. Pilot demonstration-reporting on CO_2 capture from a cement plant using hollow fiber process. *Energy Procedia* **114**, 6150–6165 (2017).
34. Adriana, R.-L., Gardarsdottir, S. O., Biermann, M., Lundqvist, K. & Harvey, S. Potential impact of the Preem CCS project. *11th Trondheim Conf. Carbon Capture, Transp. Storage* 10–18 (2021).
35. Viljoen, J. H. A., Stapelberg, F. D. J. & Cloete, M. *Technical Report on the Geological Storage of Carbon Dioxide* (2010).
36. Chabangu, N. *et al.* The investigation of CO_2 storage potential in the Algoa basin in South Africa. *Energy Procedia* **63**, 2800–2810 (2014).
37. Viebahn, P., Vallentin, D. & Höller, S. Integrated assessment of carbon capture and storage (CCS) in South Africa's power sector. *Energies* **8**, 14380–14406 (2015).
38. Viebahn, P. CCS Global final report—Part 4: Country study South Africa (2012).
39. Cloete, M. ATLAS on geological storage of carbon dioxide in South Africa 1–61 (2010).
40. Hendriks, C., Graus, W. & van Bergen, F. Global carbon dioxide storage potential and costs. *Ecofys. Utr.* **64** (2004).
41. Viebahn, P., Vallentin, D. & Höller, S. Prospects of carbon capture and storage (CCS) in China's power sector—An integrated assessment. *Appl. Energy* **157**, 229–244 (2015).
42. Viebahn, P., Vallentin, D. & Höller, S. Prospects of carbon capture and storage (CCS) in India's power sector—An integrated assessment. *Appl. Energy* **117**, 62–75 (2014).
43. European Commission. Consultative Communication on The Future of Carbon Capture and Storage in Europe (2013).
44. Zhu, L. & Fan, Y. A real options–based CCS investment evaluation model: Case study of China's power generation sector. *Appl. Energy* **88**, 4320–4333 (2011).
45. Qian, C. & Rennings, K. Low carbon scenarios vs. clean coal scenarios in China: How to close the carbon gap? In *Applied Mechanics and Materials, vols. 556–562* 841–848 (Trans Tech Publications Ltd, 2014).
46. Von Hirschhausen, C., Herold, J. & Oei, P. Y. How a 'low carbon' innovation can fail-tales from a 'lost decade' for carbon capture, transport, and sequestration (CCTS). *Econ. Energy Environ. Policy* **1**, 115–123 (2012).
47. Viebahn, P., Daniel, V. & Samuel, H. Integrated assessment of carbon capture and storage (CCS) in the German power sector and comparison with the deployment of renewable energies. *Appl. Energy* **97**, 238–248 (2012).
48. Osman, K., Coquelet, C. & Ramjugernath, D. Review of carbon dioxide capture and storage with relevance to the South African power sector. *S. Afr. J. Sci.* **110**, 1–12 (2014).
49. Chabangu, N. *et al.* The investigation of CO_2 storage potential in the Zululand Basin in South Africa. *Energy Procedia* **63**, 2789–2799 (2014).

50. Vincent, C. J. *et al.* The proposed CO_2 Test Injection project in South Africa. *Energy Procedia* **37**, 6489–6501 (2013).
51. Afolayan, B. A., Mackay, E. & Opuwari, M. 3D static modeling and CO_2 static storage estimation of the hydrocarbon-depleted Charis Reservoir, Bredasdorp Basin, South Africa. *Nat. Resour. Res.* **32**, 1021–1045 (2023).
52. Saffou, E. *et al.* Full-scale simulation of a nearly depleted gas field in South Africa for carbon utilisation and storage. *Greenh. Gases Sci. Technol.* **12**, 486–507 (2022).
53. Saffou, E. *et al.* Geomechanical characterization of CO_2 storage sites: A case study from a nearly depleted gas field in the Bredasdorp Basin, South Africa. *J. Nat. Gas Sci. Eng.* **81**, 103446 (2020).
54. Roelf, W. South Africa aims to bring pilot carbon capture project online in 2023 | Reuters. *Reuters* (2021).
55. Surridge, A. *et al.* CCUS progress in South Africa. *SSRN Electron. J.* https://doi.org/10.2139/ssrn.3820378 (2021).
56. Perkins, R. Denmark to end all North Sea oil, gas production by 2050, bans new exploration. https://www.spglobal.com/commodityinsights/en/market-insights/latest-news/natural-gas/120420-denmark-to-end-all-north-sea-oil-gas-production-by-2050-bans-new-exploration (2020).
57. State of Green. Denmark set to end all new oil and gas extraction in the North Sea by 2050. https://stateofgreen.com/en/news/denmark-set-to-end-all-new-oil-and-gas-extraction-in-the-north-sea-by-2050/ (2020).
58. Delprat-Jannaud, F. *et al.* Sitechar-methodology for a fit-for-purpose assessment of CO_2 storage sites in Europe. *Oil Gas Sci. Technol.* **70**, 531–554 (2015).
59. Orlic, B. Geomechanical effects of CO_2 storage in depleted gas reservoirs in the Netherlands: Inferences from feasibility studies and comparison with aquifer storage. *J. Rock Mech. Geotech. Eng.* **8**, 846–859 (2016).
60. Orlic, B., Heege, J. T. & Wassing, B. Assessing the integrity of fault- and top seals at CO_2 storage sites. *Energy Procedia* **4**, 4798–4805 (2011).
61. Vilarrasa, V. & Carrera, J. Geologic carbon storage is unlikely to trigger large earthquakes and reactivate faults through which CO_2 could leak. *Proc. Natl. Acad. Sci. U.S.A.* **112**, 5938–5943 (2015).
62. Siriwardane, H. J., Gondle, R. K., Varre, S. B., Bromhal, G. S. & Wilson, T. H. Geomechanical response of overburden caused by CO_2 injection into a depleted oil reservoir. *J. Rock Mech. Geotech. Eng.* **8**, 860–872 (2016).
63. Arts, R. J. *et al.* The feasibility of CO_2 storage in the depleted P18–4 gas field offshore the Netherlands (the ROAD project). *Int. J. Greenh. Gas Control* **11**, 10–20 (2012).
64. Song, Y. *et al.* Geomechanical challenges during geological CO_2 storage: A review. *Chem. Eng. J.* **456**, 140968 (2023).
65. Sander, R. Compilation of Henry's law constants, version 3.99. *Atmos. Chem. Phys. Discuss* **14**, 29615–30521 (2014).
66. Li, Y. & Nghiem, L. X. Phase equilibria of oil, gas and water/brine mixtures from a cubic equation of state and Henry's law. *Can. J. Chem. Eng.* **64**, 486–496 (1986).
67. Harvey, A. H. Semiempirical correlation for Henry's constants over large temperature ranges. *AIChE J.* **42**, 1491–1494 (1996).
68. Machida, H., Ando, R., Esaki, T., Yamaguchi, T. & Norinaga, K. Modelling of CO_2 solubility in phase separation solvent composed of amine/ether/water system for CO_2 capture. *J. Mol. Liq.* **292**, 111411 (2019).
69. Wang, G., Pickup, G., Sorbie, K. & Mackay, E. Numerical modelling of H_2 storage with cushion gas of CO_2 in subsurface porous media: Filter effects of CO_2 solubility. *Int. J. Hydrog. Energy* **47**, 28956–28968 (2022).
70. Opuwari, M. *et al.* Petrophysical core-based zonation of OW oilfield in the Bredasdorp Basin South Africa. *Sci. Rep.* **12**, 1–19 (2022).
71. Bennion, B. & Bachu, S. Relative permeability characteristics for supercritical CO_2 displacing water in a variety of potential sequestration zones. In *SPE Annual Technical Conference and Exhibition* (OnePetro, 2005).
72. Huang, J., Jin, T., Chai, Z., Barrufet, M. & Killough, J. Compositional simulation of three-phase flow in mixed-wet shale oil reservoir. *Fuel* **260**, 116361 (2020).
73. Churchwell, L., Radhakrishnan, A. & DiCarlo, D. Measurements of three-phase relative permeability as a function of fluid composition. In *Proc. SPE Symp. Improv. Oil Recover.* **2020**-*August* (2020).
74. Churchwell, L. & Dicarlo, D. Oil and gas relative permeability as a function of fluid composition. In *Proc. SPE Symp. Improv. Oil Recover.* **2022**-*April* (2022).
75. Zhou, X., Al-Otaibi, F. & Kokal, S. Relative permeability characteristics and wetting behavior of supercritical CO_2 displacing water and remaining oil for carbonate rocks at reservoir conditions. *Energy Fuels* **33**, 5464–5475 (2019).
76. Adibifard, M., Talebkeikhah, M., Sharifi, M. & Hemmati-Sarapardeh, A. Iterative Ensemble Kalman Filter and genetic algorithm for automatic reconstruction of relative permeability curves in the subsurface multi-phase flow. *J. Pet. Sci. Eng.* **192**, 107264 (2020).
77. Pham, T. H. V., Maast, T. E., Hellevang, H. & Aagaard, P. Numerical modeling including hysteresis properties for CO_2 storage in Tubåen formation, Snøhvit field, Barents Sea. *Energy Procedia* **4**, 3746–3753 (2011).
78. Pan, I., Babaei, M., Korre, A. & Durucan, S. Artificial neural network based surrogate modelling for multiobjective optimisation of geological CO_2 storage operations. *Energy Procedia* **63**, 3483–3491 (2014).
79. Eiken, O. *et al.* Lessons learned from 14 years of CCS operations: Sleipner, In Salah and Snøhvit. *Energy Procedia* **4**, 5541–5548 (2011).
80. Chiaramonte, L., White, J. A. & Trainor-Guitton, W. Probabilistic geomechanical analysis of compartmentalization at the Snøhvit CO_2 sequestration project. *J. Geophys. Res. Solid Earth* **120**, 1195–1209 (2015).
81. Ringrose, P. & Sæther, Ø. CO_2 injection operations: Insights from Sleipner and Snøhvit. in *SPE CCUS Conference* 1–14 (2020).
82. Liang, R., Fan, X., Luo, X., Sun, S. & Zhu, X. Improved IMPES scheme for the simulation of incompressible three-phase flows in subsurface porous media. *Energies* **14**, 2757 (2021).
83. Løvoll, G., Méheust, Y., Måløy, K. J., Aker, E. & Schmittbuhl, J. Competition of gravity, capillary and viscous forces during drainage in a two-dimensional porous medium, a pore scale study. *Energy* **30**, 861–872 (2005).
84. Lassen, R. N. *et al.* Effects of geologic heterogeneity on migration of gaseous CO_2 using laboratory and modeling investigations. *Int. J. Greenh. Gas Control* **43**, 213–224 (2015).
85. Qiao, Y. & Evje, S. A compressible viscous three-phase model for porous media flow based on the theory of mixtures. *Adv. Water Resour.* **141**, 103599 (2020).
86. Khan, M. Y. & Mandal, A. Analytical model for gravity segregation in WAG displacement recovery of inclined stratified reservoirs. *J. Pet. Sci. Eng.* **186**, 106722 (2020).
87. Aghabozorgi, S. & Sohrabi, M. Generalised model for simulation of two- and three-phase cycle-dependent hysteresis in sandstones. *Fuel* **310**, 122328 (2022).
88. Nygard, J. I. & Andersen, P. O. Simulation of immiscible water-alternating-gas injection in a stratified reservoir: Performance characterization using a new dimensionless number. *SPE J.* **25**, 1711–1728 (2020).
89. Black, J. R., Carroll, S. A. & Haese, R. R. Rates of mineral dissolution under CO_2 storage conditions. *Chem. Geol.* **399**, 134–144 (2015).
90. Chaves, G. *Simulation of CO2 Sequestration in Deep Saline Aquifers Simulation of CO2 Sequestration in Deep Saline Aquifers* (New Mexico Institute of Mining and Technology, 2011).
91. Lindeberg, E. Escape of CO_2 from aquifers. *Energy Convers. Manag.* **38**, S235–S240 (1997).
92. Brunet, J.-P.L., Li, L., Karpyn, Z. T. & Huerta, N. J. Fracture opening or self-sealing: Critical residence time as a unifying parameter for cement–CO_2–brine interactions. *Int. J. Greenh. Gas Control* **47**, 25–37 (2016).
93. Huerta, N. J., Hesse, M. A., Bryant, S. L., Strazisar, B. R. & Lopano, C. Reactive transport of CO_2-saturated water in a cement fracture: Application to wellbore leakage during geologic CO_2 storage. *Int. J. Greenh. Gas Control* **44**, 276–289 (2016).

94. Jian, X. & Xiaofeng, G. Assessing a potential site for offshore CO_2 storage in the Weixinan Sag in the northwestern Beibu Gulf Basin (BGB), northern South China Sea. *Greenh. Gases Sci. Technol.* https://doi.org/10.1002/ghg.2199 (2022).
95. Zhang, C., Oostrom, M., Wietsma, T. W., Grate, J. W. & Warner, M. G. Influence of viscous and capillary forces on immiscible fluid displacement: Pore-scale experimental study in a water-wet micromodel demonstrating viscous and capillary fingering. *Energy Fuels* **25**, 3493–3505 (2011).

Acknowledgements

Author contributions

B.A., E.M., and M.O. conceptualized the research. B.A. did the formal analysis and wrote the manuscript. E.M. and M.O. reviewed and edited the manuscript and figures.

Competing interests

The authors declare no competing interests.

Additional information

Correspondence and requests for materials should be addressed to B.A.

Reprints and permissions information is available at www.nature.com/reprints.

Publisher's note Springer Nature remains neutral with regard to jurisdictional claims in published maps and institutional affiliations.